

Mimicking Human Visual Development for Learning Robust Image Representations

Ankita Raj

ankita.raj@cse.iitd.ac.in

Indian Institute of Technology Delhi
New Delhi, India

Tapan Gandhi

Tapan.Kumar.Gandhi@ee.iitd.ac.in
Indian Institute of Technology Delhi
New Delhi, India

Kaashika Prajaapat

cs1170337@gmail.com

Clinikally
Gurugram, India

Chetan Arora

chetan@cse.iitd.ac.in

Indian Institute of Technology Delhi
New Delhi, India

Abstract

The human visual system is remarkably adept at adapting to changes in the input distribution—a capability modern convolutional neural networks (CNNs) still struggle to match. Drawing inspiration from the developmental trajectory of human vision, we propose a progressive blurring curriculum to improve the generalization and robustness of CNNs. Human infants are born with poor visual acuity, gradually refining their ability to perceive fine details. Mimicking this process, we begin training CNNs on highly blurred images during the initial epochs and progressively reduce the blur as training advances. This approach encourages the network to prioritize global structures over high-frequency artifacts, improving robustness against distribution shifts and noisy inputs. Challenging prior claims that blurring in the initial training epochs imposes a stimulus deficit and irreversibly harms model performance, we reveal that early-stage blurring enhances generalization with minimal impact on in-domain accuracy. Our experiments demonstrate that the proposed curriculum reduces mean corruption error (mCE) by up to 8.30% on CIFAR-10-C and 4.43% on ImageNet-100-C datasets, compared to standard training without blurring. Unlike static blur-based augmentation, which applies blurred images randomly throughout training, our method follows a structured progression, yielding consistent gains across various datasets. Furthermore, our approach complements other augmentation techniques, such as CutMix and MixUp, and enhances both natural and adversarial robustness against common attack methods. Code is available at https://github.com/rajankita/Visual_Acuity_Curriculum.

Keywords

Generalization, Robustness, Deep neural networks, Representation learning.

1 Introduction

Convolutional Neural Networks (CNNs) have achieved remarkable performance in computer vision tasks in recent years, even surpassing human performance on certain tasks. However, despite their remarkable success [35, 44], CNNs suffer from a large drop in performance when the test distribution differs from the training distribution [37]. CNNs are highly sensitive to natural image corruptions such as noise and blur [17], as well as to carefully crafted adversarial perturbations [19], limiting their reliability in real-world

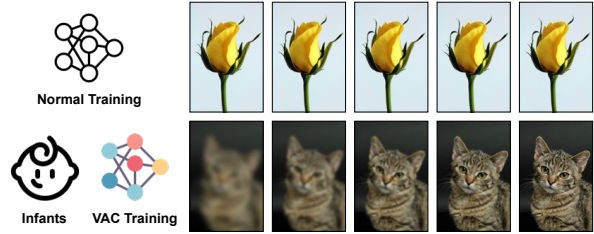


Figure 1: CNNs are trained using high resolution images from the first epoch (top row). Newborn babies, on the other hand, start with poor visual acuity and gradually develop sharper vision as their visual system matures. We propose a training curriculum, VAC, that starts with highly-blurred training images and gradually improves resolution (bottom row).

applications. In contrast, human vision is not easily disrupted by such shifts in the input distribution, suggesting fundamental differences in how humans and machines learn visual representations. This paper takes a step towards bridging this gap by identifying one such difference rooted in the developmental trajectory of human visual perception.

A growing body of work addresses CNN robustness to distribution shifts through data augmentation [12, 13], where augmented images generated by applying low-level distortions to the original data are included during training. Techniques such as AugMix [27], CutMix [58], and DeepAugment [24] employ diverse and aggressive train-time augmentations to improve robustness to natural image corruptions. While these methods have proven effective, they typically apply augmentations uniformly throughout training, without accounting for the evolving learning capacity of the model. This static treatment of input complexity may limit the model's ability to learn robust representations. Furthermore, like most work in representation learning, these techniques primarily focus on asymptotic performance in the later stages of training, overlooking the importance of early learning dynamics in shaping model robustness.

In this work, we take cues from the developmental trajectory of the human visual system to design a learning strategy for CNNs

aimed at fostering robust representations. In humans and other animals, visual acuity is initially poor at birth and gradually improves over the first few months of life [8, 50]. Neuroscientific studies suggest that initial poor retinal acuity promotes extended spatial processing in the visual cortex, which is critical for tasks such as configural face analysis [55]. Interestingly, Vogelsang *et al.* [55] observed similar effects in CNNs: training face recognition models with blurred images in the early epochs increased the effective receptive field and improved recognition performance. We extend this idea beyond face recognition and propose a generalized curriculum—Visual Acuity Learning (VAC)—that progressively transitions CNNs from low to high frequency visual input during training.

In VAC, training begins with highly blurred inputs, and the blur level is progressively reduced as training advances, ultimately reaching unaltered high-resolution images. This structured curriculum encourages the model to first attend to low-frequency, global structures before being exposed to high-frequency details. As a result, the network is less prone to overfitting on texture-level noise and spurious high-frequency artifacts. To mitigate the risk of catastrophic forgetting of the representations learned from earlier blur levels, we incorporate a replay mechanism that periodically reintroduces previous blur stages during later training phases. This mechanism not only preserves robustness acquired in earlier phases but also supports smoother adaptation to increasing image detail.

It is important to note that the proposed Visual Acuity Curriculum (VAC) differs critically from Gaussian blur augmentation. In blur augmentation, clean and blurred images are typically intermixed throughout training, exposing the network to a full spectrum of frequency information at all times. This approach lacks temporal structure and does not account for the evolving learning capacity of the model. In contrast, VAC introduces a deliberate information deficit during the early stages of training by presenting only heavily blurred inputs. This controlled progression gradually increases the level of visual detail over time. The initial period of information deficit is a key factor in our approach, as it compels the network to focus on global, low-frequency features rather than memorizing fine-grained noise. This structured exposure leads to better generalization across distribution shifts compared to static data augmentation strategies.

The proposed method offers a somewhat contrasting view to the work of Achille *et al.* [1], who argue that introducing blur in the early stages of training of a neural network induces low-level deficits, resulting in an irreversible loss in accuracy. Their work draws a parallel to the *critical learning period* observed in animals, where sensory deprivation during early development can cause permanent impairments in specific visual functions [28, 33]. We contend that this critical learning period hypothesis is incomplete. In contrast to their findings, we show that blurring in the early training stages encourages the model to learn robust, low-frequency representations, thereby improving generalization with only a marginal reduction in in-domain accuracy. For many real-world applications, this trade-off is not only acceptable, but desirable, as it yields models that are significantly more reliable in the face of real-world noise and corruption.

Contributions: We make the following contributions:

- (1) We propose VAC, a training curriculum inspired by human visual development where images are blurred in the initial epochs and progressively restored to their original form.
- (2) Through comprehensive experiments across multiple datasets and network architectures, we demonstrate that VAC improves generalization under real-world dataset shifts – evaluated using standard benchmarks for natural robustness – outperforming vanilla training and other curriculum learning methods like CBS [49] and FixRes [54].
- (3) We show that VAC is compatible with popular data augmentation techniques such as MixUp [59] and ℓ_2 -adversarial training [39], providing further improvements in generalization.
- (4) Overall, we provide a holistic perspective on the impact of blurring-based deficits in early training epochs. While the critical learning period hypothesis [1] holds so far as the in-domain accuracy is concerned, we argue that such deficits are not inherently detrimental. In fact, the marginal drop in in-domain accuracy is outweighed by a significant boost in robustness to distribution shifts.

2 Related Work

2.1 Human Visual Development and Critical Learning Period

Humans and several other animals are born with immature visual functions due to structural immaturities in the visual pathway [8, 50]. Contrast sensitivity [2, 42], visual acuity [22], orientation selectivity [6, 40], binocular vision [4, 5] and several other visual capabilities progressively improve at different rates following birth. Among these, visual acuity, which is the ability to resolve fine spatial detail, is particularly underdeveloped at birth. Newborn humans typically exhibit acuity below 20/600 [51, 55], which gradually improves to the standard adult acuity of 20/20 over the first few years.

Vogelsang *et al.* [55] hypothesize that this early period of poor acuity may not simply be a developmental limitation, but rather a functional feature that promotes the emergence of spatially extended receptive fields in the visual cortex. The reduced visual detail in early sensory input encourages spatial integration over larger regions of the visual field, helping the brain form robust, global representations of objects.

On the other hand, a few studies have shown that several visual capabilities have associated periods of enhanced plasticity, termed as ‘critical’ periods, sensory deprivation during which negatively impacts normal visual development. Following the famous experiment by Weisel and Hubel [28, 56] where the eyes of kittens were sutured to study critical periods for ocular dominance, critical periods have been observed for song learning in birds [33], and amblyopia [53] and stereopsis [14] in humans among other tasks. Analogous studies have been done for artificial neural networks as well, where researchers have shown that initial training phase plays a significant role in the performance of CNNs [15]. In their critical learning period theory for CNNs, Achille *et al.* [1] argue that stimulus deficit during the initial epochs, such as that induced by blurring of training data, results in an irrevocable loss in a network’s performance. Other works show how the optimization trajectory

of a CNN is affected by the hyperparameters of Stochastic Gradient Descent [30], learning rate [29] or regularization [18].

We believe that the findings of [1] and [55], as described above, may not be contradictory to each other. However, each may be incomplete in the sense that, whereas continuous sensory deprivation may affect accuracy, initial deprivation followed by improvement in visual acuity may be necessary to learn robust representations.

2.2 Robustness in Convolutional Neural Networks

CNNs, while excelling at large-scale vision tasks, are sensitive to input distortions. The study of robustness in CNNs covers both common image corruptions and worst-case adversarial perturbations.

Common image corruptions include diverse image degradations like noise, rain, fog, snow, and blur, etc. [17, 25, 41, 43], and is typically evaluated using the ImageNet-C [25] dataset. Geirhos *et al.* [17] pointed out that robustness to image distortions can be achieved by training on distorted images, yet it fails to generalize to previously unseen distortion types. Other methods for improving robustness to out-of-distribution data include data augmentation [24, 27, 45, 57], increasing model size, reducing texture-bias [16], pre-training on huge datasets [26], as well as combinations of these [24]. We show that VAC improves robustness to image distortions without being trained on distorted images. VAC can also be used in conjunction with these methods to further improve robustness.

Adversarial noise refers to small, imperceptible perturbations crafted using methods like FGSM [19] and PGD [39] that can drastically degrade CNN performance. Adversarial robustness techniques often rely on Adversarial Training [39] or advanced versions like TRADES [60], FSR [31], etc.

Most existing robustness techniques apply transformations statistically throughout training. In contrast, our method progressively adjusts the input resolution to guide the model toward robust feature extraction.

2.3 Curriculum Learning and Training Schedules

Curriculum learning [3] suggests that models benefit from training on easier examples first, gradually increasing task complexity. Curriculum learning by both gradually increasing the difficulty of data [20, 21], or the modeling capacity of the network [11], has been shown to improve convergence as well as performance.

Our proposed training technique can be seen as a specific instance of curriculum learning. Different from the existing approaches, in this work, we define a curriculum in terms of a blur schedule. Sinha *et al.* [49] proposed a curriculum by blurring the activation maps of convolutional layers. Unlike [49], we perform blurring of input images rather than feature maps, and are the first ones to study the impact of blurring-based deficit on generalization. Burduja *et al.* [7] proposed gradually deblurring input images to improve 3D medical image registration. Blurred images are easier to align compared to sharper images, thus their curriculum proceeds from easier to gradually more difficult concepts. On the other hand, classification using blurred images is more difficult. Thus gradually decreasing

input blur has significantly different connotations for image classification, which we address in this work. Touvron *et al.* [54] discussed the impact of the resolution of training images on test accuracy. They suggested that training with lower resolution images, and further finetuning with higher resolution images improves accuracy. Unlike [54], the proposed curriculum trains on gradually increasing image resolutions, and does not require additional fine-tuning on higher resolution images.

3 Proposed Method

Visual acuity in newborn humans and other animals develops gradually after birth, whereas CNNs are exposed to high resolution images from the very first epoch. Inspired by the findings of [55], we propose Visual Acuity Curriculum—a training routine that mimics the development of visual acuity in newborns over the first few months.

3.1 Progressive Blurring Curriculum

To simulate varying levels of visual acuity, we apply Gaussian Blur to the training images, following [55]. Prior works suggest that Gaussian blur suppresses high-frequency, texture-related components, encouraging models to focus on more global, shape-driven cues [16, 57].

Let $x \in \mathbb{R}^{H \times W \times 3}$ be a training image. The blurred version of the image is defined as:

$$\tilde{x} = \mathcal{G}_\sigma * x, \quad (1)$$

where \mathcal{G}_σ denotes a Gaussian kernel with standard deviation σ , and $*$ denotes convolution. A larger σ results in stronger blur, effectively removing high-frequency information and simulating lower visual acuity.

The training process is divided into a sequence of K curriculum segments. Each segment $k \in \{1, \dots, K\}$ is parameterized by a tuple (n_k, σ_k) , where n_k is the number of epochs and σ_k is the blur level used in that segment. To simulate the gradual improvement in acuity, we start with a high value of σ_{max} and halve σ every few epochs (refer Algorithm 1). We choose σ_{max} based on the image resolution of the training dataset, with higher σ for larger images. For convenience, σ_{max} is taken to be a power of 2. The number of epochs per segment is designed to grow exponentially, loosely mirroring the early rapid development and later gradual refinement in acuity observed in human vision [10]. We use a deficit only for the initial 20% epochs.

As an example, for the CIFAR-10 dataset with image resolution 32×32 , we train for 200 epochs starting with an initial $\sigma_{max} = 2$, with the schedule:

$$\{(13, 2), (27, 1), (160, 0)\}, \quad (2)$$

In this curriculum, the first segment of 13 epochs uses $\sigma = 2$, second segment of 27 epochs corresponds to $\sigma = 1$, and finally for the remaining 160 epochs $\sigma = 0$ is used which corresponds to using the original images (without blur) from the dataset.

3.2 Blur Replay

While the progressive blurring schedule allows the model to transition from low to high-frequency information, we observed a sharp degradation in performance on blurred inputs after transitioning to

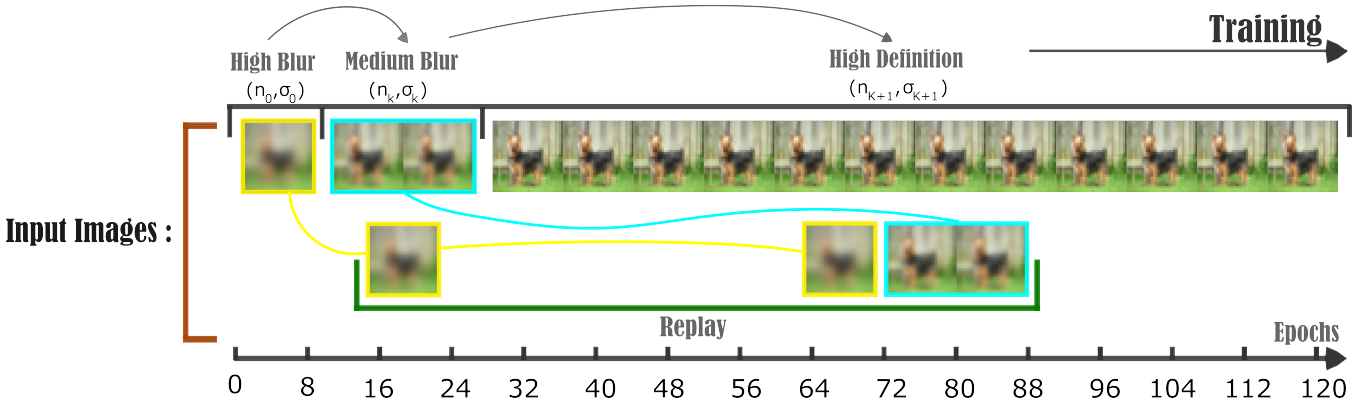


Figure 2: Visual representation of the proposed training curriculum. The entire training routine is divided into segments, each segment characterized by number of epochs n_k , and standard deviation σ_k . A segment (n_k, σ_k) includes images blurred with a Gaussian blur kernel with standard deviation σ_k as well as a replay of previously seen blur levels $\sigma_{<k}$. Training starts with highly blurred images and progresses towards sharper images.

Algorithm 1 Define curriculum

Require: Total epochs N , highest blur σ_{\max}
Ensure: $\{(n_k, \sigma_k)\}$, epochs and blur for segments of curriculum

- 1: Deficit epochs, $N_{\text{def}} = \lfloor N/5 \rfloor$ ($\lfloor \cdot \rfloor$ denotes the floor operation)
- 2: $K = \log_2(\sigma_{\max})$
- 3: $\sigma_0 = \sigma_{\max}$
- 4: $n_0 = N_{\text{def}} / \left(\sum_{i=0}^K 2^i \right)$
- 5: **for** $k = \{1, \dots, K\}$ **do**
- 6: $\sigma_k = \sigma_{k-1}/2$
- 7: $n_k = n_{k-1} \times 2$
- 8: **end for**
- 9: $\sigma_{K+1} = 0$
- 10: $n_{K+1} = N - N_{\text{def}}$

Algorithm 2 Train using VAC

Require: Training data D^{train} , Curriculum $\{(n_k, \sigma_k)\}_{k=0}^{K+1}$
Ensure: Trained model with parameters W^*

- 1: Initialize model parameters to W
- 2: **for** epoch $= \{1, \dots, \sum_{k=0}^{K+1} n_k\}$ **do**
- 3: $i \leftarrow$ index of current curriculum segment **{Line 1}**
- 4: **for** $(x, y) \in D^{\text{train}}$ **do**
- 5: $j \leftarrow$ sample from $\{0, \dots, i\}$ **{Line 2}**
- 6: $\tilde{x} = \mathcal{G}_{\sigma_j} * x$ **{Line 3}**
- 7: $\mathcal{L} \leftarrow \text{loss}(\tilde{x}, y)$
- 8: $W \leftarrow \text{update}(W, \mathcal{L})$
- 9: **end for**
- 10: **end for**
- 11: **Return** W

clean images. This is a classic symptom of catastrophic forgetting [32], wherein representations acquired in earlier training phases are overwritten by new updates.

To address this, we introduce a replay mechanism inspired by the continual learning concepts of rehearsal and memory replay

that mitigate catastrophic forgetting [32]. Specifically, we inject a fraction of training examples processed using earlier blur levels into later segments. During the initial training segment, all images are blurred using a Gaussian kernel with the maximum blur level, σ_{\max} . In subsequent segments, to prevent catastrophic forgetting of early-stage representations, we introduce a data replay mechanism. Specifically, each training image is blurred using a σ value sampled from all previously encountered blur levels. Let n_j denote the number of epochs for blur level σ_j . The sampling probability for blur level σ_j in segment k is given by:

$$p_j = \frac{n_j}{\sum_{i=1}^k n_i}, \quad \text{for } j \leq k. \quad (3)$$

This ensures that blur levels encountered earlier in the curriculum continue to be revisited proportionally in later stages, thereby reinforcing previously learned representations. As a result, the network learns to maintain robustness across a range of visual conditions rather than specializing only for high-resolution inputs. The training process for the proposed Visual Acuity Curriculum is outlined in Algorithm 2.

3.3 Implementation Simplicity

One of the practical strengths of VAC is its ease of implementation. The entire training routine can be realized with minimal changes to a standard training loop, specifically, by dynamically adjusting the blur level for each training image using a schedule and introducing a weighted sampler during the later stages. In our implementation, this requires only three additional lines of code compared to standard network training (these modifications are highlighted in Algorithm 2), making VAC compatible with most existing training pipelines.

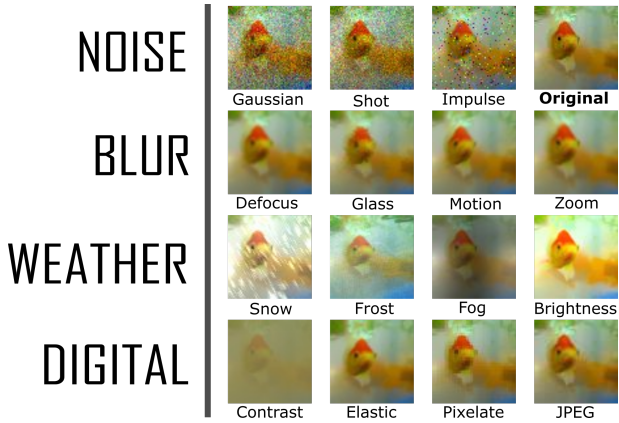


Figure 3: Examples of different image corruptions from the ImageNet-100-C dataset.

4 Experiments and Results

4.1 Experiment Setup

4.1.1 *Datasets*. We use two RGB image datasets for our experiments. CIFAR-10 dataset [34] comprises of 32×32 low-resolution images belonging to 10 object classes, with 50,000 training and 10,100 testing images. ImageNet-100 [36] is a larger dataset with 224×224 images, which is a subset of the original ImageNet dataset [46], obtained by sampling every tenth class from the original dataset.

4.1.2 *Corruption Datasets*. To evaluate performance under distribution shift, we use common corruption benchmarks [25]: CIFAR-10-C, and ImageNet-100-C. These are corrupted versions of the test sets of CIFAR-10 and ImageNet-100 respectively, comprising of images distorted with 15 types of corruptions frequently encountered in natural images, broadly grouped into four classes: Noise, Blur, Weather and Digital (Figure 3). Each corruption type has 5 levels of severity, amounting to a total of 75 different corruptions. These corruptions do not include Gaussian Blur, thus there is no conflict with Gaussian blurring used during training.

4.1.3 *Metrics*. *Clean error* is the top-1 error reported on the standard test set for each of the datasets. Following previous work, we report *mean Corruption Error (mCE)* [25] for corruption datasets, computed by averaging the top-1 errors across all corruptions and severity levels on the corruption datasets.

4.1.4 *Training Details*. Unless otherwise mentioned, we use PreAct ResNet-18 architecture [23], and train it for 200 epochs on CIFAR-10 and 100 epochs on ImageNet-100. All networks are trained from scratch. The curricula used for training with VAC on the two datasets are noted below.

$$\begin{array}{ll} \text{CIFAR-10:} & \{(13, 2), (27, 1), (160, 0)\} \\ \text{ImageNet-100:} & \{(1, 8), (3, 4), (5, 2), (11, 1), (80, 0)\} \end{array}$$

The designed curricula ensure that the epochs summed over all segments of a curriculum equals the number of epochs for its vanilla training counterpart.

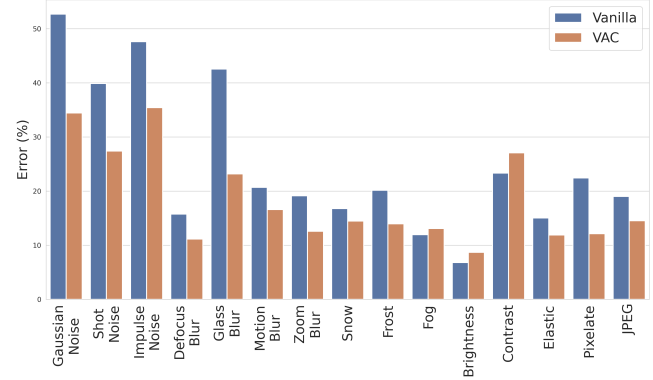


Figure 4: Robustness under data shift: mean Corruption Error across 15 types of image corruptions. Each bar shows the corruption error averaged over 5 severity levels. VAC reduces error (improves accuracy) over most corruption types.

4.2 Improvement in Common Corruption Robustness

To evaluate the effectiveness of the proposed VAC, we compare it against *vanilla training*, defined as the conventional training of models on clean, high-resolution images from the beginning, without any blur-based curriculum. As shown in Table 1, VAC consistently improves robustness to common corruptions across different neural network architectures, including both classical models like ResNet-18 and more modern architectures such as ConvNeXt [38]. This suggests that the benefits of VAC are not architecture-specific and can generalize across different model families.

Although VAC leads to a noticeable reduction in mean corruption error (mCE), we observe a small increase in clean (in-domain) error compared to standard training. This trade-off reflects the well-known tension between robustness and clean accuracy. Interestingly, our findings also offer a counterpoint to the Critical Learning Period hypothesis proposed by Achille *et al.* [1], which suggests that early exposure to degraded input (such as blur) leads to irreversible accuracy loss. While we do observe a slight drop in clean performance, our results indicate that this early-stage information deficit actually promotes more generalizable representations, enabling the network to perform better under distribution shifts.

To better understand the source of these robustness gains, we present a detailed breakdown of corruption types in Figure 4 for a ResNet-18 trained on CIFAR-10. We find that VAC-trained models outperform their vanilla counterparts on most corruption types, including noise-based corruptions (Gaussian noise, impulse noise), weather distortions (snow, frost), and blur-based corruptions (defocus blur, glass blur). These improvements are particularly notable because the model is never explicitly trained on these corruptions.

However, VAC underperforms on a few corruption categories, most notably brightness and contrast perturbations. We hypothesize that this may be due to the proposed curriculum removing the sparse details which were present in the low-light images. On the other hand, human visual system adapts to low light through an entirely different mechanism not covered in the curriculum.

Table 1: Clean error and mean Corruption Errors (mCE) of vanilla training compared with VAC. Lower error values are better. Displayed values for CIFAR-10 are the mean error values over 3 repetitions for each entry, expressed as %. For ImageNet-100, we report results from a single run for each experiment.

Dataset	Architecture	Vanilla training		Visual Acuity Curriculum	
		Clean error (↓)	mCE (↓)	Clean error (↓)	mCE (↓)
CIFAR-10	All-Conv [52]	6.13	31.19	6.77	27.83
	ResNet-18 [23]	5.24	25.03	6.92	18.78
	ResNet-56 [23]	6.55	28.67	10.37	20.37
	MobileNet-v2 [47]	14.66	33.03	16.90	29.60
	ConvNeXt [38]	7.07	17.00	7.66	16.39
ImageNet-100	ResNet-18 [23]	13.12	53.66	15.24	49.23
	ResNet-50 [23]	10.96	51.86	15.98	49.03

Incorporating such mechanisms, or combining VAC with a photometrically adaptive or multi-scale strategy, could further enhance performance on these challenging corruptions. We leave this as an avenue for future work.

We also note that VAC adds negligible training overhead: training a ResNet-18 on CIFAR-10 with VAC takes 3768s vs. 3729s with vanilla training on an NVIDIA V100 GPU. Importantly, VAC only affects training time; inference speed remains unchanged.

4.3 Comparison with other Training Strategies

We now compare the proposed VAC with a selection of established training strategies that aim to improve either generalization, robustness, or learning dynamics. Specifically, we evaluate against FixRes [54], Curriculum by Smoothing (CBS) [49], and SuperLoss [9] – three methods with differing motivations and mechanisms.

FixRes [54] focuses on scale consistency by decoupling resolution from input size and has been shown to improve clean accuracy in high-resolution classification tasks. CBS [49] implements curriculum learning by gradually increasing the sharpness of network activations using activation smoothing. SuperLoss [9], on the other hand, adaptively reweights the training loss based on sample difficulty, helping the network to avoid overfitting to noisy or outlier samples.

We perform an evaluation of each method across two key robustness benchmarks: corruption robustness using the CIFAR-10-C dataset, and adversarial robustness under a standard PGD (Projected Gradient Descent) [39] attack with $\epsilon = 2/255$. The results are summarized in Table 2. VAC outperforms all competing strategies in terms of corruption robustness, achieving the lowest mCE across the board. While FixRes and SuperLoss achieve moderate improvements in clean test accuracy, they show limited or even negative impact on robustness. In some cases, both corruption and adversarial performance degrade relative to vanilla training. This suggests that strategies optimized purely for clean performance may inadvertently compromise the model’s resilience to input distribution shifts or adversarial perturbations.

CBS is the only competing method that provides a clear improvement in adversarial robustness, achieving a reduced attack success rate (ASR) under PGD. However, its effectiveness on natural corruptions is limited, and in our experiments, VAC outperforms CBS in terms of mCE. Notably, both VAC and CBS involve a form of

curriculum learning, yet the nature of what is being “smoothed” differs fundamentally. CBS smooths internal activations, whereas VAC manipulates the input signal in a biologically motivated way. Our results suggest that manipulating the input signal via Gaussian blur yields more pronounced improvements in robustness to real-world corruptions, possibly because it imposes an inductive bias that encourages the learning of spatially coherent, low-frequency representations.

An interesting finding is that although VAC is not explicitly designed to defend against adversarial attacks, it still improves adversarial robustness over vanilla training, FixRes and SuperLoss. This suggests that the early information deficit enforced by VAC may lead to more stable and noise-tolerant features, which are less susceptible to perturbations, adversarial or otherwise.

4.4 Compatibility with Data Augmentation

One of the strengths of the proposed curriculum is its compatibility with a wide range of existing data augmentation strategies. Rather than acting as a replacement, VAC is designed to complement these methods, offering a biologically inspired inductive bias that enhances representation learning. Many recent advances in robustness rely on augmentations that introduce variation in the training distribution, such as spatial manipulations, pixel-level mixing, or adversarial perturbations. VAC can be easily integrated with these approaches to further improve robustness.

To demonstrate compatibility, we combine VAC with five widely-used data augmentation strategies: MixUp [59], CutMix [58], Adversarial Training [39], RandAugment [13], and AutoAugment [12]. Each of these methods addresses robustness through different mechanisms: MixUp performs convex combinations of images and labels to smooth decision boundaries, CutMix replaces regions of an image with patches from another to enhance spatial generalization, Adversarial Training explicitly incorporates adversarial examples to defend against gradient-based attacks, while RandAugment and AutoAugment operate by learning or randomly sampling from a large search space of augmentation policies to create a more varied and robust training distribution.

Our integration procedure is simple and preserves the design intent of each method. For a given augmentation (e.g., MixUp), we first apply Gaussian blur to the input image according to the current VAC curriculum stage. The blurred images are then passed

Table 2: Comparison of VAC with other training strategies, evaluated for a ResNet-18 network trained on CIFAR-10. We report clean error and common corruption errors (%) and Attack Success Rate (ASR) for PGD adversarial attack.

Method	Clean error (\downarrow)	Mean CE (\downarrow)	ASR (\downarrow)
Vanilla Training	5.43	24.60	54.31
FixRes [54]	5.49	27.21	59.24
CBS [49]	5.79	27.87	46.23
SuperLoss [9]	5.74	27.07	58.44
VAC (Proposed)	6.63	17.58	50.37

Table 3: Performance of VAC combined with data augmentation techniques on a ResNet-18 trained on CIFAR-10. We report clean error, common corruption error, and Attack Success Rate (ASR) under a PGD adversarial attack.

Method	Clean error (\downarrow)	Mean CE (\downarrow)	ASR (\downarrow)
MixUp [59]	4.40	19.00	68.01
MixUp + VAC	5.68	18.66	57.89
CutMix [58]	4.14	28.90	73.55
CutMix + VAC	4.87	21.99	69.39
ℓ_2 adversarial [39]	6.24	16.29	21.01
ℓ_2 adversarial + VAC	9.01	15.82	21.36
RandAugment [13]	4.97	18.77	52.06
RandAugment + VAC	6.08	14.59	49.04
AutoAugment [12]	4.78	18.21	52.82
AutoAugment + VAC	6.07	15.04	45.79

through the selected augmentation pipeline. This ordering reflects the natural perceptual sequence in humans, where low-resolution global structure is processed first, followed by exposure to diverse contextual variations.

As shown in Table 3, combining VAC with these augmentation strategies leads to further improvements in both common corruption robustness and adversarial robustness. These results support our hypothesis that VAC introduces a complementary inductive bias that improves the effectiveness of existing data augmentations, and can serve as a general-purpose module in robustness-focused training pipelines, particularly when combined with augmentation strategies that introduce orthogonal forms of variability.

4.5 Ablation Study

The proposed curriculum is motivated by the developmental trajectory of the human visual system, which gradually improves visual acuity over time. While this inspiration provides a compelling biological basis, our final curriculum design involves several heuristics and practical choices. In this section, we perform an ablation study to assess the effect of these design decisions.

Table 4: Ablation study. Clean and corruption errors (%) on ResNet-18 trained on CIFAR-10, for alternative training regimens.

Method	Clean error (\downarrow)	Mean CE (\downarrow)
VAC (Proposed)	6.63	17.58
Linear curriculum	7.07	17.99
Inverse curriculum	14.95	35.98
Continuous curriculum	6.33	20.28
Steep (no replay)	20.21	23.52
Constant blur 100%	67.67	68.16
Constant blur 20%	6.18	18.02

4.5.1 Curriculum variants. Firstly, we compare VAC with several curriculum variants and blur-based baselines in Table 4: (i) **Linear Curriculum**: This tests whether an evenly spaced progression is as effective as our proposed exponential decay. The schedule is defined as $\{(20, 2), (20, 1), (160, 0)\}$, where the blur level decreases in equal-duration steps. (ii) **Inverse Curriculum**: Defined as $\{(13, 0), (27, 1), (160, 2)\}$, this curriculum starts with clean images and increases blur over time. It serves as a counter-hypothesis to test whether early access to detailed features provides any robustness benefit. (iii) **Continuous Curriculum**: Here, we fix the blur level at $\sigma = 2$ and gradually reduce the proportion of blurred images in each mini-batch over time, rather than staging the transition in discrete segments. This tests whether blur quantity, rather than sharp transition boundaries, is the critical factor. (iv) **Steep Curriculum (No Replay)**: A simplified schedule defined as $\{(20, 2), (180, 0)\}$ that makes a sharp transition from high blur to clean inputs without incorporating replay. This variant is used to isolate the effect of the replay mechanism introduced in VAC. (v) **Constant Blur**: We test two cases: one where 100% of inputs in every batch are blurred using $\sigma = 2$, and another with 20% blurred inputs. These serve as baselines for conventional blur-based augmentation without curriculum structure.

The results indicate that the choice and scheduling of blur exposure significantly impact both clean and corruption robustness. The *inverse curriculum*, which delays the introduction of blur until later training epochs, yields the worst corruption and clean error, confirming that late-stage deficits harm representational fidelity. Similarly, applying high blur uniformly throughout training (*constant blur at 100%*) leads to degraded performance, suggesting that excessive visual suppression limits the model’s ability to learn fine-grained discriminative features. The *steep curriculum* variant, which drops blur abruptly after the initial phase without replay, suffers from markedly high clean error. This supports our hypothesis that catastrophic forgetting erodes representations learned during the initial blurred phase unless earlier inputs are periodically replayed. The sharp drop in performance underlines the necessity of our replay mechanism. While *linear* and *continuous* curricula provide reasonable trade-offs, they fall short of the performance achieved by the proposed schedule. Notably, the proposed exponential decay schedule with replay achieves the best balance between clean accuracy and corruption robustness.

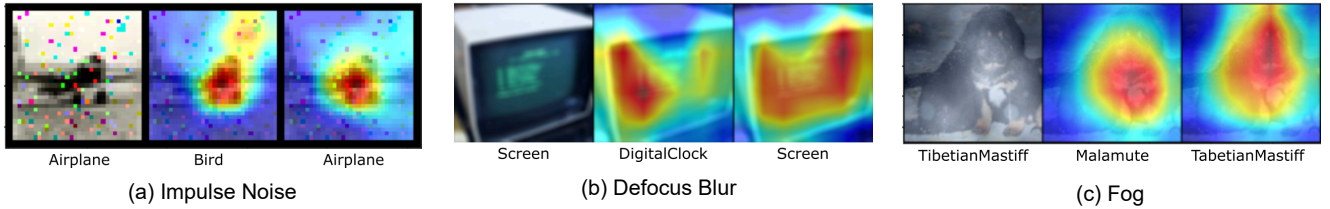


Figure 5: Grad-CAM visualizations: (a) shows image from CIFAR-10, and (b) and (c) from ImageNet-100. Each set shows results for a particular image corruption. First column in a set is the corrupted image, second and third columns are the Grad-CAMs created for Vanilla and VAC trained networks respectively. Original and predicted labels are depicted below the images. The discriminative regions in the CAM output are larger and more pronounced for VAC.

This ablation study thus validates several key aspects of our design: the importance of starting with high blur, reducing blur progressively rather than abruptly, and reinforcing earlier blur levels via replay. These components collectively contribute to the effectiveness of VAC in learning robust representations.

4.5.2 Deficit period. The choice of 20% deficit epochs ($N_{\text{def}} = \lfloor N/5 \rfloor$ in Algorithm 1) is based on empirical evaluation. Increasing the deficit in the range of 5% to 40% reduces corruption error (19% to 17.3%) but increases clean error to 9.02%, with diminishing returns after 30%. The 20% deficit balances clean and corruption errors well.

4.5.3 Guidance on choosing σ_{max} . The choice of σ_{max} depends on input resolution: we use $\sigma_{\text{max}} = 2$ for 32×32 and $\sigma_{\text{max}} = 8$ for 224×224 images. Larger σ_{max} increases initial blur, impacting clean accuracy more than mCE. For example, on ImageNet-100 with ResNet-18, increasing σ_{max} from 4 to 8 to 16 raises clean error from 14.18% to 15.24% and 17.48%. We recommend tuning σ_{max} via grid search based on image size to balance robustness and accuracy.

4.5.4 Deficit vs. Data Augmentation. The proposed method creates a sensory deficit by exposing the network to *only* low resolution images in the early epochs. A close alternative to the proposed curriculum is the commonly used blur-based Data Augmentation, where blurred images are *intermixed* with clean images over the entire training period, represented by the *constant blur 20%* method in Table 4. Constant blur 20% achieves lower clean error compared to VAC, which can be attributed to the fact that there is no deficit enforced in the initial epochs. However, VAC achieves lower corruption error, suggesting the benefits of stimulus deficit in the early epochs compared to regular data augmentation with blurred images.

4.6 Grad-CAM Visualizations

To better understand the qualitative differences in feature representations learned by models trained with the Visual Acuity Curriculum (VAC), we employ Grad-CAM [48] to visualize class-discriminative regions in the input images. Figure 5 presents comparisons between models trained with VAC and those trained via standard (vanilla) procedures on examples drawn from the CIFAR-10 and ImageNet-100 datasets.

We observe that, under a variety of image degradations, such as blur, noise, or fog, the Grad-CAM maps from VAC-trained networks tend to focus on broader and more semantically meaningful

regions of the image. In contrast, vanilla-trained models often localize on narrow or fragmented regions, many of which do not clearly correspond to object-specific features.

These visualizations support our hypothesis that the early-stage information deficit imposed by VAC encourages the model to rely on coarse, low-frequency features and global structural cues. As a result, the network learns to extract more spatially coherent and resilient representations that generalize better under distribution shifts. The broader activation patterns suggest that VAC-trained models are less prone to overfitting on fine-grained, potentially spurious details in the training data.

5 Conclusion and Future Work

We proposed a training curriculum for neural networks inspired by the gradual development of visual acuity in human infants. Our experiments show that this biologically motivated approach enhances the robustness of CNNs against a wide range of unseen image corruptions and distribution shifts. Rather than replacing existing robustness techniques, our method is complementary, offering a new inductive bias grounded in human vision. By simulating an early-stage sensory deficit and gradually increasing input detail during training, we aim to bridge a small but meaningful gap between biological and artificial visual learning. Our findings suggest that such developmental priors can guide networks toward more generalizable and resilient representations.

This work opens several promising avenues for future research. Other aspects of human visual development, such as the progressive emergence of color perception or binocular depth processing, may also provide useful principles for designing training curricula. Another exciting direction is to study how the proposed curriculum interacts with vision transformers (ViTs), which, unlike CNNs, rely on self-attention mechanisms to model global context. Investigating whether gradually increasing input resolution improves ViT robustness and sample efficiency could lead to broader insights into curriculum design for modern architectures.

Acknowledgments

The authors would like to thank Soumen Basu, Ashutosh Agarwal, Devesh Pant and Gaurav Talebailkar for their help in carrying out some of the experiments.

References

- [1] Alessandro Achille, Matteo Rovere, and Stefano Soatto. 2018. Critical learning periods in deep networks. In *International Conference on Learning Representations*.
- [2] Janette Atkinson, Oliver Braddick, and Kathleen Moar. 1977. Contrast sensitivity of the human infant for moving and static patterns. *Vision Research* 17, 9 (1977), 1045–1047.
- [3] Yoshua Bengio, Jérôme Louradour, Ronan Collobert, and Jason Weston. 2009. Curriculum learning. In *Proceedings of the 26th annual international conference on machine learning*, 41–48.
- [4] Eileen Birch and Benno Petrig. 1996. FPL and VEP measures of fusion, stereopsis and stereoacuity in normal infants. *Vision research* 36, 9 (1996), 1321–1327.
- [5] Eileen E Birch, Jane Gwiazda, and Richard Held. 1982. Stereoacuity development for crossed and uncrossed disparities in human infants. *Vision research* 22, 5 (1982), 507–513.
- [6] OJ Braddick, J Wattam-Bell, and J Atkinson. 1986. Orientation-specific cortical responses develop in early infancy. *Nature* 320, 6063 (1986), 617–619.
- [7] Mihai Burduja and Radu Tudor Ionescu. 2021. Unsupervised medical image alignment with curriculum learning. In *2021 IEEE International Conference on Image Processing (ICIP)*. IEEE, 3787–3791.
- [8] Andreas Burkhalter, Kerry L Bernardo, and Vinod Charles. 1993. Development of local circuits in human visual cortex. *Journal of Neuroscience* 13, 5 (1993), 1916–1931.
- [9] Thibault Castells, Philippe Weinzaepfel, and Jerome Revaud. 2020. Superloss: A generic loss for robust curriculum learning. *Advances in Neural Information Processing Systems* 33 (2020), 4308–4319.
- [10] A Chandra. 1991. Natural history of the development of visual acuity in infants. *Eye* 5, 1 (1991), 20–26.
- [11] Florinel-Alin Croitoru, Nicolae-Catalin Ristea, Radu Tudor Ionescu, and Nicu Sebe. 2022. LeRaC: Learning Rate Curriculum. *arXiv preprint arXiv:2205.09180* (2022).
- [12] Ekin D Cubuk, Barret Zoph, Dandelion Mane, Vijay Vasudevan, and Quoc V Le. 2019. Autoaugment: Learning augmentation strategies from data. In *Proceedings of the IEEE/CVF conference on computer vision and pattern recognition*, 113–123.
- [13] Ekin D Cubuk, Barret Zoph, Jonathon Shlens, and Quoc V Le. 2020. Randaugment: Practical automated data augmentation with a reduced search space. In *Proceedings of the IEEE/CVF conference on computer vision and pattern recognition workshops*, 702–703.
- [14] Sherry L Fawcett, Yi-Zhong Wang, and Eileen E Birch. 2005. The critical period for susceptibility of human stereopsis. *Investigative ophthalmology & visual science* 46, 2 (2005), 521–525.
- [15] Jonathan Frankle, David J Schwab, and Ari S Morcos. 2020. The early phase of neural network training. *arXiv preprint arXiv:2002.10365* (2020).
- [16] Robert Geirhos, Patricia Rubisch, Claudio Michaelis, Matthias Bethge, Felix A Wichmann, and Wieland Brendel. 2018. ImageNet-trained CNNs are biased towards texture; increasing shape bias improves accuracy and robustness. In *International Conference on Learning Representations*.
- [17] Robert Geirhos, Carlos R Medina Temme, Jonas Rauber, Heiko H Schütt, Matthias Bethge, and Felix A Wichmann. 2018. Generalisation in humans and deep neural networks. In *NeurIPS*.
- [18] Aditya Golatkar, Alessandro Achille, and Stefano Soatto. [n. d.]. Time Matters in Regularizing Deep Networks: Weight Decay and Data Augmentation Affect Early Learning. ([n. d.]).
- [19] Ian J Goodfellow, Jonathon Shlens, and Christian Szegedy. 2014. Explaining and harnessing adversarial examples. *arXiv preprint arXiv:1412.6572* (2014).
- [20] Alex Graves, Marc G. Bellemare, Jacob Menick, Rémi Munos, and Koray Kavukcuoglu. 2017. Automated Curriculum Learning for Neural Networks. In *Proceedings of the 34th International Conference on Machine Learning (Proceedings of Machine Learning Research, Vol. 70)*, Doina Precup and Yee Whye Teh (Eds.). PMLR, 1311–1320. <https://proceedings.mlr.press/v70/graves17a.html>
- [21] Guy Hacohen and Daphna Weinshall. 2019. On The Power of Curriculum Learning in Training Deep Networks. In *Proceedings of the 36th International Conference on Machine Learning (Proceedings of Machine Learning Research, Vol. 97)*, Kamalika Chaudhuri and Ruslan Salakhutdinov (Eds.). PMLR, 2535–2544. <https://proceedings.mlr.press/v97/hacohen19a.html>
- [22] Russell D Hamer, Anthony M Norcia, Christopher W Tyler, and Charlene Hsu-Winges. 1989. The development of monocular and binocular VEP acuity. *Vision Research* 29, 4 (1989), 397–408.
- [23] Kaiming He, Xiangyu Zhang, Shaoqing Ren, and Jian Sun. 2016. Identity mappings in deep residual networks. In *Computer Vision–ECCV 2016: 14th European Conference, Amsterdam, The Netherlands, October 11–14, 2016, Proceedings, Part IV* 14. Springer, 630–645.
- [24] Dan Hendrycks, Steven Basart, Norman Mu, Saurav Kadavath, Frank Wang, Evan Dorundo, Rahul Desai, Tyler Zhu, Samyak Parajuli, Mike Guo, Dawn Song, Jacob Steinhardt, and Justin Gilmer. 2021. The Many Faces of Robustness: A Critical Analysis of Out-of-Distribution Generalization. *ICCV* (2021).
- [25] Dan Hendrycks and Thomas Dietterich. 2018. Benchmarking Neural Network Robustness to Common Corruptions and Perturbations. In *International Conference on Learning Representations*.
- [26] Dan Hendrycks, Kimin Lee, and Mantas Mazeika. 2019. Using pre-training can improve model robustness and uncertainty. In *International Conference on Machine Learning*. PMLR, 2712–2721.
- [27] Dan Hendrycks, Norman Mu, Ekin Dogus Cubuk, Barret Zoph, Justin Gilmer, and Balaji Lakshminarayanan. 2019. AugMix: A Simple Data Processing Method to Improve Robustness and Uncertainty. In *International Conference on Learning Representations*.
- [28] David H Hubel and Torsten N Wiesel. 1970. The period of susceptibility to the physiological effects of unilateral eye closure in kittens. *The Journal of physiology* 206, 2 (1970), 419–436.
- [29] Stanislaw Jastrzebski, Devansh Arpit, Oliver Astrand, Giancarlo B Kerg, Huan Wang, Caiming Xiong, Richard Socher, Kyunghyun Cho, and Krzysztof J Geras. 2021. Catastrophic fisher explosion: Early phase fisher matrix impacts generalization. In *International Conference on Machine Learning*. PMLR, 4772–4784.
- [30] Stanislaw Jastrzebski, Maciej Szymczak, Stanislav Fort, Devansh Arpit, Jacek Tabor, Kyunghyun Cho, and Krzysztof Geras. 2019. The Break-Even Point on Optimization Trajectories of Deep Neural Networks. In *International Conference on Learning Representations*.
- [31] Woo Jae Kim, Yoonki Cho, Junsik Jung, and Sung-Eui Yoon. 2023. Feature separation and recalibration for adversarial robustness. In *Proceedings of the IEEE/CVF conference on computer vision and pattern recognition*, 8183–8192.
- [32] James Kirkpatrick, Razvan Pascanu, Neil Rabinowitz, Joel Veness, Guillaume Desjardins, Andrei A Rusu, Kieran Milan, John Quan, Tiago Ramalho, Agnieszka Grabska-Barwinska, et al. 2017. Overcoming catastrophic forgetting in neural networks. *Proceedings of the national academy of sciences* 114, 13 (2017), 3521–3526.
- [33] Masakazu Konishi. 1985. Birdsong: from behavior to neuron. *Annual review of neuroscience* 8, 1 (1985), 125–170.
- [34] Alex Krizhevsky et al. 2009. Learning multiple layers of features from tiny images. (2009).
- [35] Alex Krizhevsky, Ilya Sutskever, and Geoffrey E Hinton. 2012. Imagenet classification with deep convolutional neural networks. *Advances in neural information processing systems* 25 (2012), 1097–1105.
- [36] Cassidy Laidlaw, Sahil Singla, and Soheil Feizi. 2020. Perceptual adversarial robustness: Defense against unseen threat models. *arXiv preprint arXiv:2006.12655* (2020).
- [37] Da Li, Yongxin Yang, Yi-Zhe Song, and Timothy M Hospedales. 2017. Deeper, broader and artier domain generalization. In *Proceedings of the IEEE international conference on computer vision*, 5542–5550.
- [38] Zhuang Liu, Hanzi Mao, Chao-Yuan Wu, Christoph Feichtenhofer, Trevor Darrell, and Saining Xie. 2022. A convnet for the 2020s. In *Proceedings of the IEEE/CVF Conference on Computer Vision and Pattern Recognition*, 11976–11986.
- [39] Aleksander Madry, Aleksandar Makelov, Ludwig Schmidt, Dimitris Tsipras, and Adrian Vladu. 2018. Towards Deep Learning Models Resistant to Adversarial Attacks. In *International Conference on Learning Representations*.
- [40] M Concetta Morrone and David C Burr. 1986. Evidence for the existence and development of visual inhibition in humans. *Nature* 321, 6067 (1986), 235–237.
- [41] Yaniv Ovadia, Emily Fertig, Jie Ren, Zachary Nado, D Sculley, Sebastian Nowozin, Joshua Dillon, Balaji Lakshminarayanan, and Jasper Snoek. 2019. Can you trust your model’s uncertainty? Evaluating predictive uncertainty under dataset shift. *Advances in Neural Information Processing Systems* 32 (2019), 13991–14002.
- [42] Mario Pirchio, Donatella Spinelli, Adriana Fiorentini, and Lamberto Maffei. 1978. Infant contrast sensitivity evaluated by evoked potentials. *Brain Research* (1978).
- [43] Benjamin Recht, Rebecca Roelofs, Ludwig Schmidt, and Vaishaal Shankar. 2019. Do imagenet classifiers generalize to imagenet? In *International Conference on Machine Learning*. PMLR, 5389–5400.
- [44] Shaoqing Ren, Kaiming He, Ross Girshick, and Jian Sun. 2015. Faster r-cnn: Towards real-time object detection with region proposal networks. *Advances in neural information processing systems* 28 (2015), 91–99.
- [45] Evgenia Rusak, Lukas Schott, Roland S Zimmermann, Julian Bitterwolf, Oliver Bringmann, Matthias Bethge, and Wieland Brendel. 2020. A simple way to make neural networks robust against diverse image corruptions. In *European Conference on Computer Vision*. Springer, 53–69.
- [46] Olga Russakovsky, Jia Deng, Hao Su, Jonathan Krause, Sanjeev Satheesh, Sean Ma, Zhiheng Huang, Andrej Karpathy, Aditya Khosla, Michael Bernstein, Alexander C. Berg, and Li Fei-Fei. 2015. ImageNet Large Scale Visual Recognition Challenge. *International Journal of Computer Vision (IJCV)* 115, 3 (2015), 211–252. doi:10.1007/s11263-015-0816-y
- [47] Mark Sandler, Andrew Howard, Menglong Zhu, Andrey Zhmoginov, and Liang-Chieh Chen. 2018. Mobilenetv2: Inverted residuals and linear bottlenecks. In *Proceedings of the IEEE conference on computer vision and pattern recognition*, 4510–4520.
- [48] Ramprasaath R Selvaraju, Michael Cogswell, Abhishek Das, Ramakrishna Vedantam, Devi Parikh, and Dhruv Batra. 2017. Grad-cam: Visual explanations from deep networks via gradient-based localization. In *Proceedings of the IEEE international conference on computer vision*, 618–626.

- [49] Samarth Sinha, Animesh Garg, and Hugo Larochelle. 2020. Curriculum by smoothing. *Advances in Neural Information Processing Systems* 33 (2020), 21653–21664.
- [50] Caitlin R Siu and Kathryn M Murphy. 2018. The development of human visual cortex and clinical implications. *Eye and brain* 10 (2018), 25.
- [51] Samuel Sokol. 1978. Measurement of infant visual acuity from pattern reversal evoked potentials. *Vision research* 18, 1 (1978), 33–39.
- [52] Jost Tobias Springenberg, Alexey Dosovitskiy, Thomas Brox, and Martin Riedmiller. 2014. Striving for simplicity: The all convolutional net. *arXiv preprint arXiv:1412.6806* (2014).
- [53] David Taylor et al. 1979. Critical period for deprivation amblyopia in children. *Transactions of the ophthalmological societies of the United Kingdom* 99, 3 (1979), 432–439.
- [54] Hugo Touvron, Andrea Vedaldi, Matthijs Douze, and Hervé Jégou. 2019. Fixing the train-test resolution discrepancy. *Advances in neural information processing systems* 32 (2019).
- [55] Lukas Vogelsang, Sharon Gilad-Gutnick, Evan Ehrenberg, Albert Yonas, Sidney Diamond, Richard Held, and Pawan Sinha. 2018. Potential downside of high initial visual acuity. *Proceedings of the National Academy of Sciences* 115, 44 (2018), 11333–11338.
- [56] Torsten N Wiesel and David H Hubel. 1963. Effects of visual deprivation on morphology and physiology of cells in the cat's lateral geniculate body. *Journal of neurophysiology* 26, 6 (1963), 978–993.
- [57] Dong Yin, Raphael Gontijo Lopes, Jon Shlens, Ekin Dogus Cubuk, and Justin Gilmer. 2019. A Fourier Perspective on Model Robustness in Computer Vision. *Advances in Neural Information Processing Systems* 32 (2019), 13276–13286.
- [58] Sangdoo Yun, Dongyoon Han, Seong Joon Oh, Sanghyuk Chun, Junsuk Choe, and Youngjoon Yoo. 2019. Cutmix: Regularization strategy to train strong classifiers with localizable features. In *Proceedings of the IEEE/CVF International Conference on Computer Vision*. 6023–6032.
- [59] Hongyi Zhang, Moustapha Cisse, Yann N Dauphin, and David Lopez-Paz. 2018. mixup: Beyond Empirical Risk Minimization. In *International Conference on Learning Representations*.
- [60] Hongyang Zhang, Yaodong Yu, Jiantao Jiao, Eric Xing, Laurent El Ghaoui, and Michael Jordan. 2019. Theoretically principled trade-off between robustness and accuracy. In *International conference on machine learning*. PMLR, 7472–7482.